Article

Cell Reports

MiR-980 Is a Memory Suppressor MicroRNA that Regulates the Autism-Susceptibility Gene *A2bp1*

Graphical Abstract

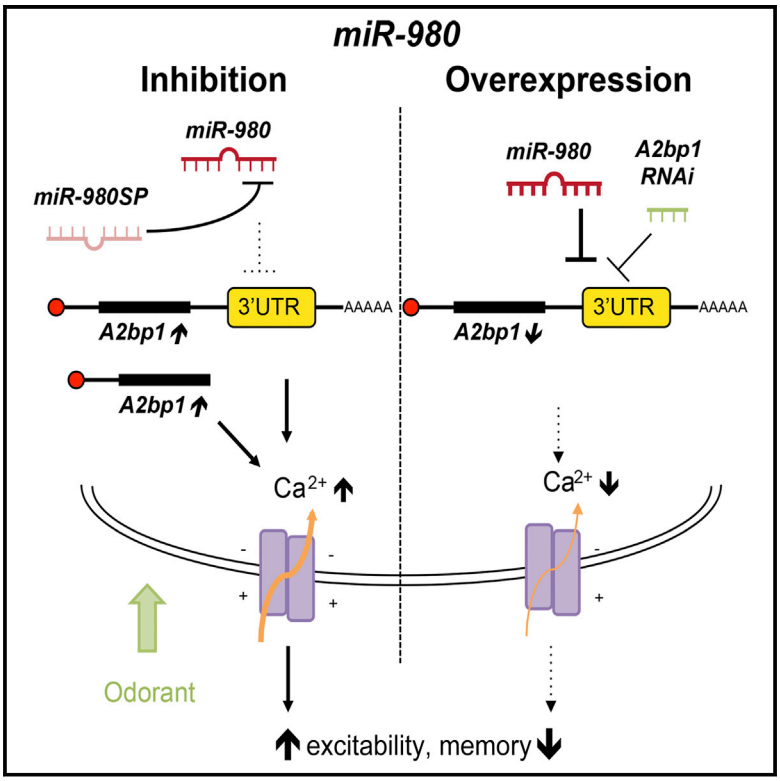

Highlights

- *Drosophila miR-980* inhibition enhances olfactory memory; *miR-980* overexpression impairs olfactory memory
- *miR-980* inhibition in multiple areas of the adult brain enhances memory
- *miR-980* modulates odor-induced calcium responses and excitability in the adult brain
- *miR-980* represses A2bp1 expression in the adult brain; reducing A2bp1 expression reverses the memory enhancement due to *miR-980* inhibition

Authors

Tugba Guven-Ozkan, Germain U. Busto, Soleil S. Schutte, Isaac Cervantes-Sandoval, Diane K. O'Dowd, Ronald L. Davis

Correspondence

rdavis@scripps.edu

In Brief

The *microRNA-980* gene functions to suppress olfactory learning and memory formation by regulating the activity of the autism-susceptibility gene, *A2bp1*. Overexpression of *A2bp1* enhances memory and is therefore termed a memory-promoting gene. The memory enhancing effects of *microRNA-980* suppression appear to occur through altering excitability of neurons in the olfactory nervous system.

Accession Numbers

KU315475

Guven-Ozkan et al., 2016, Cell Reports *14*, 1698–1709
February 23, 2016 ©2016 The Authors
http://dx.doi.org/10.1016/j.celrep.2016.01.040

OPEN ACCESS
CellPress

Cell Reports
Article

MiR-980 Is a Memory Suppressor MicroRNA that Regulates the Autism-Susceptibility Gene *A2bp1*

Tugba Guven-Ozkan,[1,4] Germain U. Busto,[1,4] Soleil S. Schutte,[2,3] Isaac Cervantes-Sandoval,[1] Diane K. O'Dowd,[2,3] and Ronald L. Davis[1,*]

[1]Department of Neuroscience, The Scripps Research Institute Florida, Jupiter, FL 33458, USA
[2]Department of Developmental and Cell Biology, University of California, Irvine, Irvine, CA 92697, USA
[3]Department of Anatomy and Neurobiology, University of California, Irvine, Irvine, CA 92697, USA
[4]Co-first author
*Correspondence: rdavis@scripps.edu
http://dx.doi.org/10.1016/j.celrep.2016.01.040

SUMMARY

MicroRNAs have been associated with many different biological functions, but little is known about their roles in conditioned behavior. We demonstrate that *Drosophila miR-980* is a memory suppressor gene functioning in multiple regions of the adult brain. Memory acquisition and stability were both increased by *miR-980* inhibition. Whole cell recordings and functional imaging experiments indicated that *miR-980* regulates neuronal excitability. We identified the autism susceptibility gene, *A2bp1*, as an mRNA target for *miR-980*. A2bp1 levels varied inversely with *miR-980* expression; memory performance was directly related to A2bp1 levels. In addition, *A2bp1* knockdown reversed the memory gains produced by *miR-980* inhibition, consistent with *A2bp1* being a downstream target of *miR-980* responsible for the memory phenotypes. Our results indicate that *miR-980* represses *A2bp1* expression to tune the excitable state of neurons, and the overall state of excitability translates to memory impairment or improvement.

INTRODUCTION

MicroRNAs (miRNAs) are small (21–23 nt), non-coding RNAs that repress gene expression to regulate cellular development and physiology (Ambros, 2004). A short seed sequence (6–8 nt) located at the 5′ end of miRNAs binds to complementary sequences in the 3′-UTR of target mRNAs to repress mRNA expression by blocking translation and/or promoting degradation of the mRNA target (Lee et al., 1993; Wightman et al., 1993; Bartel and Chen, 2004; Bartel, 2009; McNeill and Van Vactor, 2012). Thus, miRNAs offer a relatively rapid, analog, and cell-type-specific control mechanism for the epigenetic expression of genomic information in both time and space (Kosik, 2006; McNeill and Van Vactor, 2012).

One aspect of miRNA function that remains understudied concerns the roles for these molecules in learning and memory, a primary adaptive function of the CNS. Prior studies revealed that broad insults to the miRNA processing pathway impairs memory formation in both *Drosophila* and the mouse (Ashraf et al., 2006; Konopka et al., 2010; Schaefer et al., 2010; Bredy et al., 2011). Although eukaryotic genomes encode hundreds of distinct miRNAs and they are generally expressed at high levels in the CNS, only a handful of specific miRNAs have been studied and implicated in memory formation through roles in neuronal maturation, connectivity, and synaptic plasticity (Bredy et al., 2011; McNeill and Van Vactor, 2012; Li et al., 2013; Saab and Mansuy, 2014).

To identify the miRNAs that participate in the biology of memory formation, we conducted a large scale, comprehensive screen using a transgenic approach to systematically inhibit 134 different miRNAs (Busto et al., 2015), using a "microRNA sponge" technique (Ebert et al., 2007; Loya et al., 2009). We surveyed the influences of 134 miRNAs for effects on intermediate term (ITM, i.e., at 3 hr after conditioning), olfactory aversive memory. From this screen, we identified several new miRNAs that function to inhibit or promote memory formation at this time point (Busto et al., 2015). *MiR-980*, when inhibited, was shown to enhance memory formation. Thus, *MiR-980*, a member of the *miR-22* family of vertebrate miRNAs (Ruby et al., 2007), was classified as having a memory suppressor function.

Here, we characterize the memory suppressing function of *miR-980*. Among the mRNA targets for *miR-980*, we demonstrate that the autism-susceptibility gene, Ataxin2 binding protein 1 (*A2bp1*, also known as Rbfox-1, Fox-1) is a primary target responsible for *miR-980*-directed memory suppression. A2bp1 is a known RNA binding protein involved in alternative splicing of a network of critical neuronal genes during development and in adults (Lee et al., 2009; Fogel et al., 2012) and in addition to autism (ASD), is associated with intellectual disability and epilepsy (Bhalla et al., 2004; Martin et al., 2007; Sebat et al., 2007; Mikhail et al., 2011; Davis et al., 2012). Opposite to the role for *miR-980*, we identify *A2bp1* as a memory-promoting gene. Our combined data advance our understanding of the *miR-22* family of miRNAs, showing that in *Drosophila* the magnitude of memory formation is a direct function of *miR-980* abundance and of its primary mRNA target for this function, A2bp1.

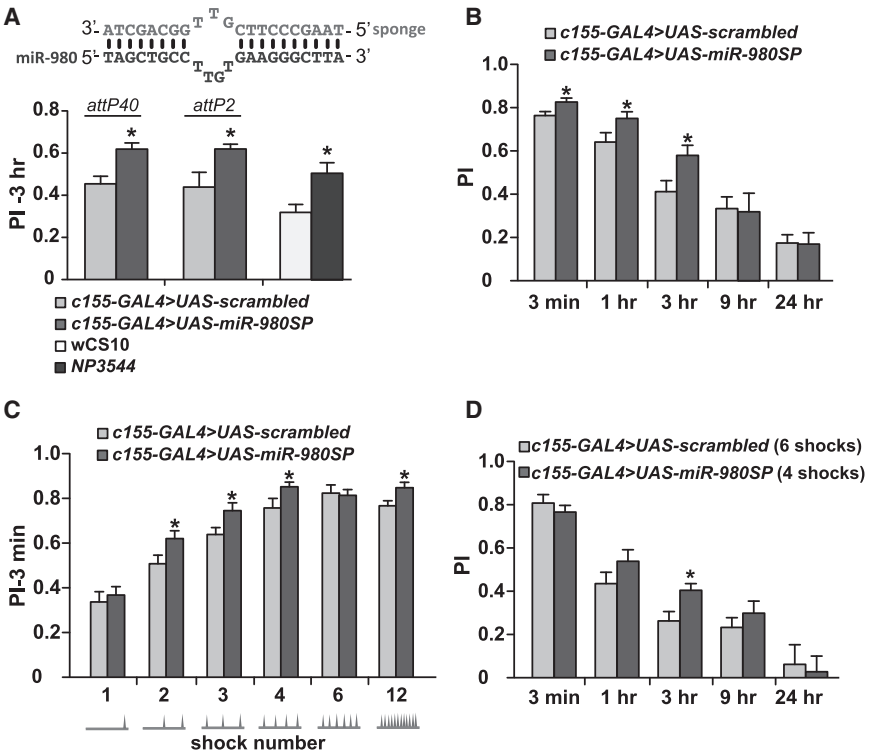

Figure 1. *MiR-980* Inhibition Enhances Olfactory Memory by Potentiating Acquisition and Memory Stability

(A) *MiR-980* inhibition enhances 3 hr aversive memory. The *miR-980* targeting sponge contains sequence mismatches to prevent RNA-interference-mediated degradation of the sponge RNA (Ebert et al., 2007). Two independent *UAS-miR-980SP* insertions, in the *attP40* (second chromosome) and *attP2* (third chromosome) sites, and the hypomorphic *miR-980* mutant *NP3544* improve 3 hr memory. The *UAS-miR-980* sponge expression was driven by the pan-neuronal *c155-GAL4* element; transgenic lines containing scrambled sequences (*UAS-scrambled)* were used as controls. PI, performance index. Statistics: experimental and control groups were compared by the two-tailed, two-sample Student's t test. $p < 0.01$ for *attP40* and *NP3544* line, $p < 0.05$ for *attP2* insert. PIs are the mean ± SEM with $n \geq 6$.

(B) Decay of aversive olfactory memory. *miR-980* inhibition enhances 3 min, 1 hr, and 3 hr memory. 3 min, 1 hr, 3 hr, 9 hr, and 24 hr memory was tested for *UAS-miR-980SP* and *UAS-scrambled* flies containing the *c155-GAL4* driver. Statistics: the *c155-GAL4>UAS-miR-980SP* PI at each time point was compared to the *c155-GAL4>UAS-scrambled* PI on different days and compared using a two-tailed, two-sample Student's t tests for each time point. $p < 0.05$. PIs are the mean ± SEM with $n \geq 6$.

(C) *MiR-980* inhibition enhances memory acquisition. Three-minute memory of *c155-GAL4>UAS-scrambled* and *c155-GAL4>UAS-miR-980SP* flies was tested after 1, 2, 3, 4, 6, and 12 shock training with a 1min CS+ odor presentation. Shock delivery is schematized below each condition. Statistics: PIs for each shock treatment were tested on different days and were analyzed by two-tailed, two-sample Student's t tests for each condition. $p < 0.05$ for 2, 3, 4, and 12 shock treatments. PIs are the mean ± SEM with $n = 8$.

(D) *MiR-980* memory retention with a normalized initial PI. Three min PIs of *scrambled* and *miR-980SP* flies were normalized with six or four shocks, respectively during CS+ odor exposure. Memory was tested at 3 min, 1 hr, 3 hr, 9 hr, and 24 hr on different days. Statistics: PIs were compared using two-tailed, two-sample Student's t tests for each time point. $p < 0.05$ for 3 hr memory. PIs are the mean ± SEM with $n = 8$.

See also Figure S1.

RESULTS

MiR-980 Inhibition Enhances Olfactory Learning and Memory Stability

We recently tested 3 hr olfactory memory of 134 *Drosophila* miRNA sponge lines (Fulga et al., 2015) using the pan-neuronal driver *c155-GAL4* (Busto et al., 2015). Expression of the *miR-980* targeting sponge (*UAS-miR-980SP*) surprisingly enhanced the memory performance index (PI) (Figure 1A) by ~40% compared to the UAS-scrambled control flies, without significantly altering odor or shock avoidance (Figure S1A). Two separate *miR-980SP* transgenes, one inserted at the *attP40* locus (second chromosome) and the other at the *attP2* locus (third chromosome), both significantly enhanced 3 hr PIs compared to their respective *UAS-scrambled* controls (Figure 1A). We also tested *NP3544* flies, which have a P-element in the *miR-980* gene reducing its expression by 64% in fly heads as measured by qRT-PCR (Marrone et al., 2012; and data not shown) ($p < 0.01$, $n = 3$). The *NP3544* hypomorph also enhanced 3 hr memory compared to the *wCS10* control flies without altering odor and shock avoidance (Figure S1B); reinforcing the conclusion that *miR-980* normally functions in memory suppression (Figure 1A).

Memory time course experiments showed that expression of *miR-980SP* enhanced 3 min, 1 hr, and 3 hr memory but not 9 hr or 24 hr memory (Figure 1B). The effect on immediate performance after conditioning suggested that *miR-980SP* expression might enhance learning. To test acquisition, flies were trained with an increasing number of shock pulses during a 1 min CS+ odor presentation followed by a 1 min CS− odor (Figure 1C). Memory tested immediately after training with two, three, or four shocks was enhanced, consistent with the conclusion that inhibition of *miR-980* improves the acquisition of the odor:shock contingency (Figure 1C). We also normalized initial PI scores for *scrambled* and *miR-980SP* groups by training the former with six and the latter with four shocks (Figure 1D). Although initial performance was similar between the two groups, memory expressed by *miR-980SP* flies was significantly enhanced at 3 hr, revealing an additional role in the suppression of memory stability (Figure 1D).

MiR-980 Enhances Memory When Inhibited during Adulthood in Multiple Areas of the CNS

To distinguish whether *miR-980* inhibition enhances memory due to developmental changes or roles in adult physiology, we restricted the temporal expression of the *miR-980SP* transgene

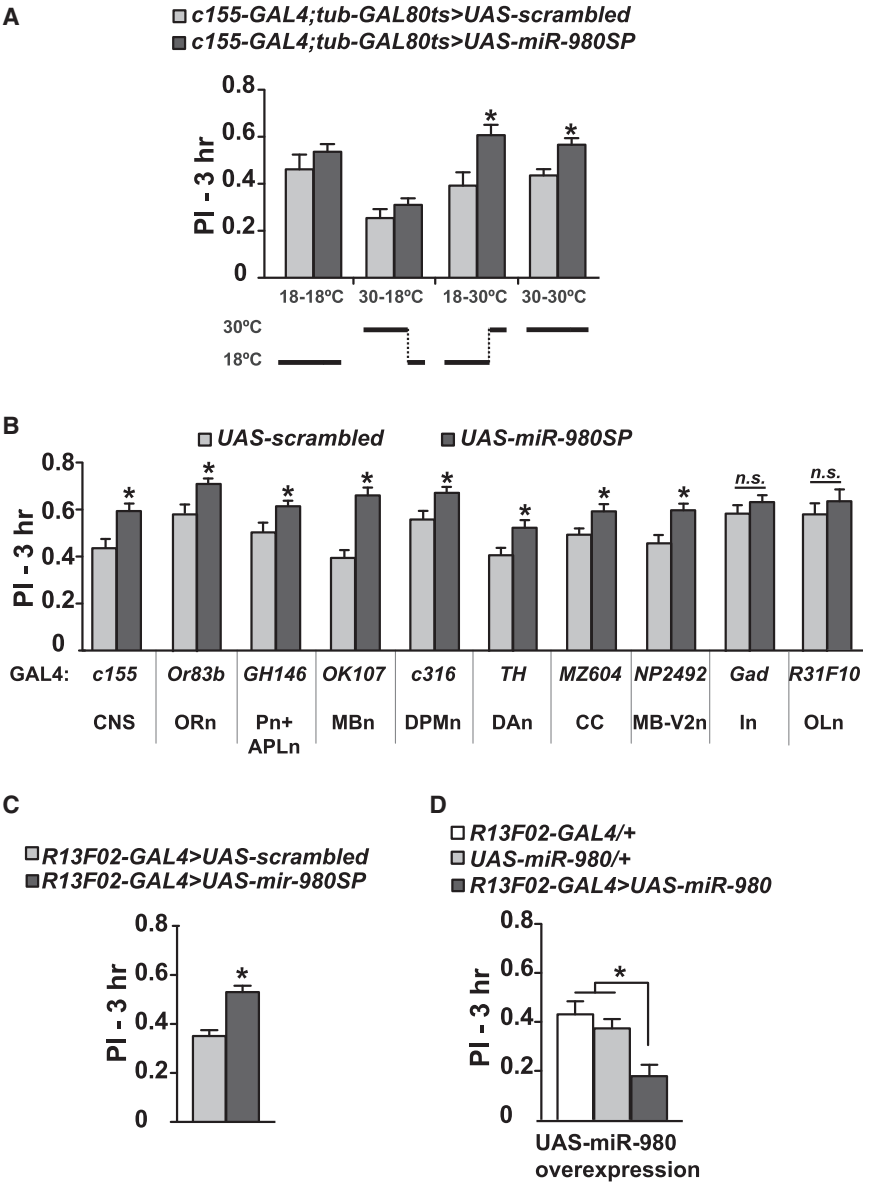

Figure 2. Memory Enhancement Occurs from Inhibiting *miR-980* in Multiple Areas of the CNS during Adulthood

(A) Memory enhancement occurs from *miR-980* inhibition during adulthood. The *c155-GAL4* expression was modulated during development and adulthood using *tub-GAL80^{ts}*, with temperature shifts schematized below the bar graph. Flies expressing the *scrambled* control sequence using *c155-GAL4;tub-GAL80^{ts}* were used as the control for 3 hr aversive memory. Statistics: PIs were analyzed by two-tailed, two-sample Student's t tests for each condition. $p < 0.01$ for flies kept at 18°C during development and 30°C during adulthood and for flies kept at 30°C during both development and adulthood. PIs are the mean ± SEM with $n \geq 10$.

(B) *MiR-980SP* spatial mapping. The *UAS-scrambled* and *UAS-miR-980SP* flies were crossed to a battery of *GAL4* lines that drive expression in specific populations of neurons. The *c155-GAL4* driver was used as the positive control. The GAL4 drivers used and their abbreviated expression domains are shown below the graph. ORn, olfactory receptor neurons; Pn, projection neurons; APLn, anterior paired lateral neuron; MBn, mushroom body neurons; DPMn, dorsal paired medial neuron; DAn, dopaminergic neurons; CC, central complex; MB-V2n, mushroom body V2 neuron; In, inhibitory neurons; OLn, optic lobe neurons. Statistics: PIs were analyzed by two-tailed, two-sample Student's t tests for each driver compared to the scrambled crosses. $p < 0.05$ for *miR-980SP* crossed to *GH146-GAL4*, *c316-GAL4*, *TH-GAL4*, *MZ604-GAL4*; $p < 0.01$ for *c155-GAL4*, *Or83b-GAL4*, *NP2492-GAL4;* and $p < 0.0001$ for *OK107-GAL4*. PIs are the mean ± SEM with $n \geq 16$.

(C) *MiR-980SP* expression in the MB using another GAL4 driver, *R13F02-GAL4*, improved 3 hr memory consistent with *OK107-GAL4* results. Flies were conditioned with three shocks during the 1min CS+ odor representation to avoid ceiling scores. Statistics: PIs were analyzed by two-tailed, two-sample Student's t test. $p < 0.05$. PIs are the mean ± SEM with $n = 8$.

(D) Overexpression of *miR-980* in MB impairs 3 hr memory. Statistics: 3 hr olfactory memory of *R13F02-GAL4>UAS-miR-980* flies was compared to *GAL4*-only and *UAS*-only controls using one-way ANOVA followed by Bonferroni's post hoc tests. PIs are the mean ± SEM with $n = 12$. $p < 0.01$.
See also Figures S1 and S2.

using the TARGET system (McGuire et al., 2003). With this system, GAL4 function is repressed in the presence of a temperature-sensitive GAL80 protein (*tub-GAL80^{ts}*) at the permissive temperature (18°C) and derepressed at the restrictive temperature (30°C). There was no difference in memory scores between control and experimental flies maintained at 18°C throughout the experiment (Figure 2A). Similarly, *miR-980* inhibition only during development produced no difference between control and experimental groups (Figure 2A). In contrast, *miR-980* inhibition throughout development and adulthood—or only during adulthood—produced the enhanced memory phenotype (Figure 2A). Therefore, the enhancement of memory occurs from *miR-980SP* expression during adulthood.

Many types of neurons within the *Drosophila* olfactory nervous system mediate memory acquisition, consolidation, forgetting, and retrieval (Guven-Ozkan and Davis, 2014). Olfactory receptor neurons (ORn) detect the odorants (CS+/CS−) and transmit this olfactory information to the antennal lobe (AL). Projection neurons (Pn) originating within the AL then convey the information to the mushroom body neurons (MBn). Neuromodulatory neurons, like dopamine neurons (DAn) are thought to convey the US (shock) stimulus to MBn. The CS and US stimuli are integrated in the MBn, one "center" for olfactory memory (Davis, 2005, 2011). Other MB extrinsic neurons that modulate memory formation include the anterior paired lateral neurons (APLn), dorsal paired medial neurons (DPMn), neurons in the central

complex (CC), and MB-V2n (Guven-Ozkan and Davis, 2014). We employed *GAL4* lines that promote expression in these and other neurons to identify the sets of neurons that respond to *miR-980* inhibition by enhancing memory. Surprisingly, *miR-980* inhibition improved 3 hr memory using all *GAL4* lines tested except for *Gad-GAL4*, which drives expression in GABAergic inhibitory neurons, and *R31F10-GAL4*, which drives expression in optic lobe neurons (Figure 2B). To avoid a possible masking effect due to a ceiling on memory performance, *miR-980* inhibition using *Gad-GAL4* and *R31F10-GAL4* was tested using a milder training protocol, but this failed to improve memory scores (Figures S2A and S2B). These data indicate that *miR-980* functions as a memory suppressor gene in multiple areas of the adult brain and more specifically, in excitatory neurons that generally are part of the olfactory nervous system.

We tested odor and shock avoidance of *miR-980* inhibition using various drivers including *GH146-GAL4*, *OK107-GAL4*, *238Y-GAL4*, and *R13F02-GAL4* (Figures S1C–S1F; data not shown). Many of the drivers we tested with *miR-980SP* showed enhanced sensitivity to odors or shock. A MB-specific driver, *R13F02-GAL4* that also enhances memory (Figure 2C), was the only driver identified other than *c155-GAL4* with no significant odor and shock avoidance difference between the control and the sponge-expressing flies (Figure S1F). One explanation for the memory enhancement with broad spatial *miR-980* suppression along with increased overall odor and shock sensitivity is that neurons in the experimental flies may be more excitable. This hypothesis was tested with experiments presented below.

MiR-980 Overexpression in the Mushroom Bodies Impairs 3 Hr Memory

Since reducing *miR-980* expression enhanced memory expression, we wondered whether its overexpression might impair expression. *MiR-980* overexpression using *c155-GAL4* produced pupal lethality. Therefore, we tested the effects of increasing *miR-980* expression by driving *UAS-miR-980* with the more specific MBn driver, *R13F02-GAL4* (Bejarano et al., 2012). Opposite to and consistent with the phenotype observed with *miR-980* inhibition, overexpression in the MBn impaired 3 hr memory relative to the *GAL4*-only and *UAS*-only controls (Figure 2D). Memory impairment observed upon overexpression of *miR-980* cannot be attributed to impaired odor or shock perception (Figure S1G). Thus, we conclude that *MiR-980* expression has a bidirectional influence on memory performance.

MiR-980 Bidirectionally Influences Naive Odor Responses of Mushroom Body Neurons and Neuronal Excitability

MB responses to odors presented to the fly can be detected by monitoring calcium influx into these neurons (Wang et al., 2001; Yu et al., 2006; Turner et al., 2008). To test whether *miR-980* expression might influence the response of MBn when odorants are presented to the fly, we recorded Ca^{2+} responses using GCaMP3 in naive flies exposed to octanol (oct) or benzaldehyde (ben), the two odorants we used for conditioning. The Ca^{2+} responses to octanol and benzaldehyde were increased in both the vertical and horizontal lobes of the MBn of the *miR-980SP*-expressing flies, and decreased in the *miR-980*-overexpressing flies compared to the *UAS-scrambled* control (Figure 3A). These results reveal that the quantitative representation of odors in the MB is inversely related to *miR-980* expression. This relationship is consistent with the hypothesis that *miR-980* normally suppresses neuronal excitability.

To evaluate the effect of *miR-980* on neuronal excitability, whole cell recordings were performed using adult brain projection neurons (Pn). Pn of 2-day-old adult female flies expressing *scrambled*, *miR-980SP*, and *miR-980* with the *GH146-GAL4* driver were recorded blind with respect to genotype. Depolarizing current injections were used to measure the intrinsic firing properties in the presence of the synaptic blockers curarine and picrotoxin with all cells held at −65 mV. There was no significant difference in holding current, input resistance, or cell capacitance in the scrambled control, *miR-980SP*, and *miR-980* overexpression flies.

Supra-threshold current injections evoked depolarizations capped by a train of small amplitude spikelets characteristic of sodium-dependent action potentials (Figure 3B). The spikelet frequency in the scrambled control was consistent with that of wild-type Pn (Iniguez et al., 2013). The mean firing frequency was significantly different among the scrambled control, *miR-980SP*, and *miR-980* overexpression lines. The *miR-980SP* Pn exhibited a significantly higher firing frequency than the scrambled control at current steps between 80–100 pAs. The mean firing frequency was not significantly different between the *miR-980* overexpression and the scrambled control Pn (Figure 3B), although there was a clear difference in the shape of the input-output curve and *miR-980* overexpressing Pn exhibited a strong trend for lower mean firing frequency at 40–50 pA, which may indicate a role in inhibiting excitability. Nonetheless, *miR-980SP* data demonstrate that *miR-980* modulates the excitability of Pn with a clearly increased excitability when *miR-980* is inhibited, consistent with the GCaMP3 imaging experiments.

The Autism-Susceptibility Gene, *A2bp1*, Is a Target of *miR-980*

We used bioinformatic prediction software to obtain insights into the potential mRNA targets of *miR-980* and then tested the functional relevance of those genes to memory formation, initially using an RNAi knockdown approach. Using TargetScan (http://Targetscan.org) and microRNA.org (http://microRNA.org) bioinformatics tools, we identified 95 mRNA targets with a possible role in the *miR-980* phenotype. Fifty-eight of the predicted target genes with an available RNAi line from the VDRC KK library (Dietzl et al., 2007) were previously tested for 3 hr memory using *nSyb-GAL4*, a pan-neuronal driver (Table S1) (Walkinshaw et al., 2015). Given the bidirectional regulation of memory performance with overexpression or inhibition of *miR-980*, it seemed possible that RNAi knockdown of true targets might expose a memory phenotype. A direct relationship between miRNA expression level, target mRNA expression level, and phenotype predicts that knockdown of a repressive miRNA by a miRNA-SP transgene should produce an elevated level of mRNA target. The phenotype obtained by RNAi knockdown of an authentic mRNA target may thus be opposite to that obtained with a miRNA-SP transgene and in the same direction as *miR-980* overexpression.

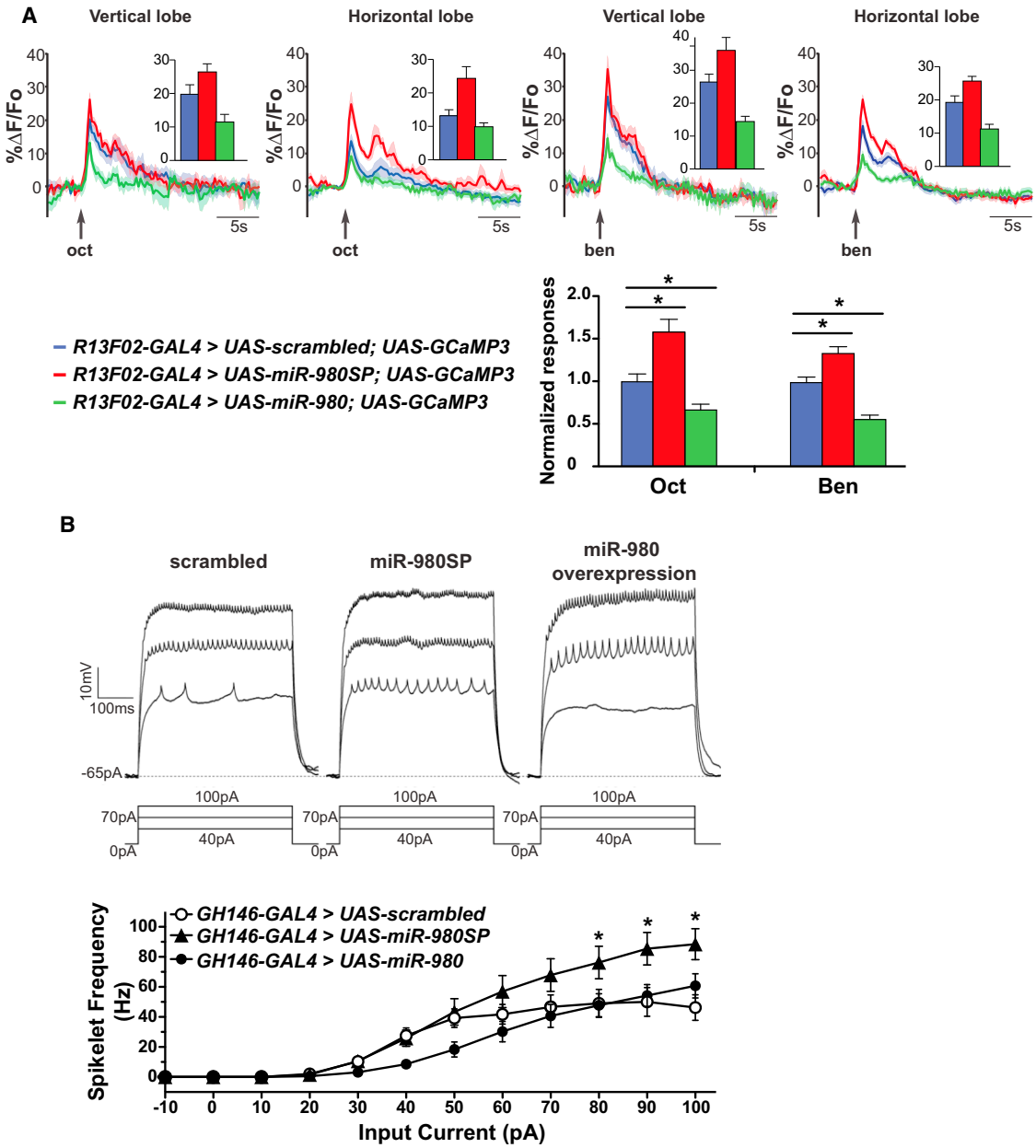

Figure 3. *MiR-980* Expression Modulates the Excitable State of Neurons

(A) Recording of odor evoked Ca^{2+} influx in the vertical and horizontal MB lobes. GCaMP3 fluorescence was recorded while 3 s of octanol (oct)- or benzaldehyde (ben)-laced air was applied to *R13F02-GAL4>UAS-scrambled*, *R13F02-GAL4>UAS-miR-980SP*, and *R13F02-GAL4>UAS-miR-980* overexpressing flies. The graphs show the sliding mean of the $\Delta F/F_o$ as a function of time, with the SEM represented as the shaded outline. Group data quantifying the peak response from baseline are shown as insets. Oct and ben responses in the vertical and horizontal lobes were normalized and averaged. The *R13F02-GAL4>UAS-miR-980SP* flies exhibited elevated odor evoked Ca^{2+} responses compared to the *UAS-scrambled* control. The *R13F02-GAL4>UAS-miR-980* overexpression flies exhibited impaired odor evoked Ca^{2+} responses. Statistics: responses were analyzed using one-way ANOVA followed by Bonferroni's post hoc tests. Results are the mean ± SEM with n = 12. $p < 0.0001$.

(B) *MiR-980* modulates the excitability of projection neurons (Pn) in adult antennal lobes. Representative current clamp recordings of *GH146-GAL4>UAS-scrambled* control, *GH146-GAL4>UAS-miR-980SP* and *GH146-GAL4>UAS-miR-980* overexpression Pn are shown. Spikelet frequency is plotted as a function of the current step. The firing frequency from *miR-980SP* Pn was significantly higher than the scrambled control at higher current steps. The mean firing frequency from *miR-980* overexpression Pn was not significantly different with the scrambled control Pn, although a strong trend was observed at 40–50 pA. Statistics: mean firing frequencies were analyzed using two-way ANOVA followed by Bonferroni's post hoc tests. Results are the mean ± SEM with n = 21 for scrambled, n = 19 for *miR-980SP* and *miR-980* overexpression. $p < 0.001$.

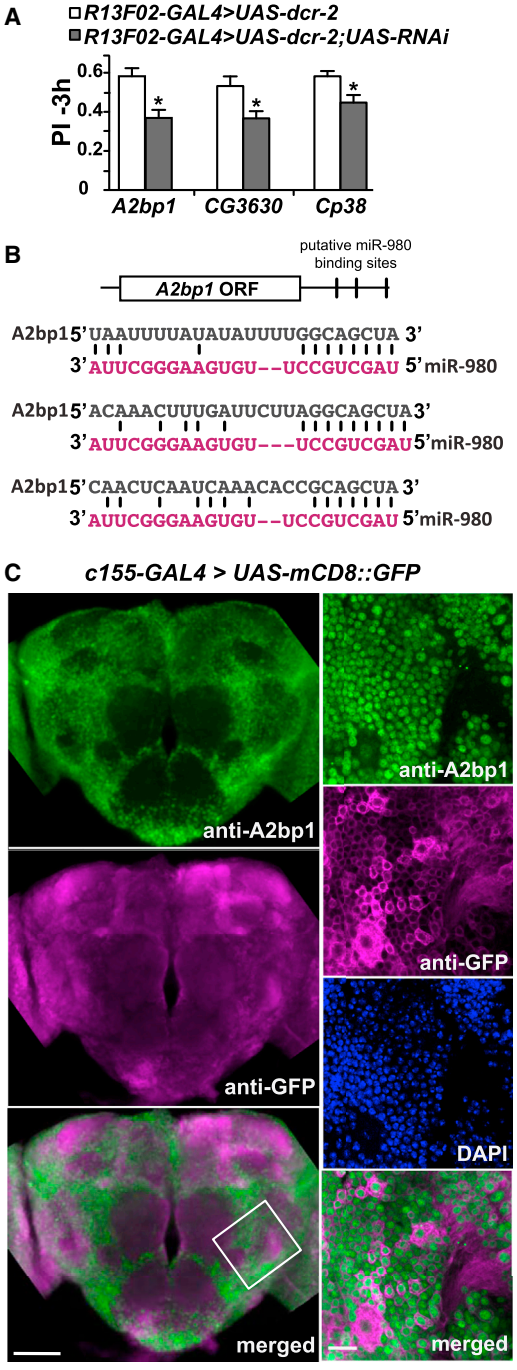

Figure 4. RNAi Screen for Potential *miR-980* Target Genes Identified the Autism-Susceptibility Gene, *A2bp1*

(A) Three of the *miR-980* predicted target genes impair 3 hr memory using an RNAi approach. Predicted *miR-980* target genes were screened using RNAis expressed in the MB with *R13F02-GAL4;UAS-dcr-2*. Three-hour memory scores for three of the final hits compared to the *R13F02-GAL4>UAS-dcr-2* control are shown. Statistics: PIs were analyzed by two-tailed, two-sample Student's t tests. $p < 0.01$ for *A2bp1 RNAi*, $p < 0.05$ for *CG3630* and *Cp38 RNAi*. PIs are the mean ± SEM with n = 10.

(B) Schematic diagram of the *A2bp1* mRNA showing the location of three predicted *miR-980* binding sites in the 3′ UTR. Sequences that are complementary between *miR-980* and *A2bp1* 3′ UTR are illustrated.

(C) A2bp1 is broadly expressed and primarily localized to nuclei in the *Drosophila* brain. Representative maximum intensity projection images of anti-A2bp1 (green) and anti-GFP (magenta) immunostaining of the central brain of *c155-GAL4>mCD8::GFP* flies. The bottom panel shows the merged image for the anti-A2bp1 and anti-GFP images. Scale bar, 50 μm. The panels to the right show high-magnification images of a 3-μm single slice of the brain area identified by the white-bordered square in the merged image. Anti-A2bp1 (green), anti-GFP (magenta), DAPI (blue) and the merged image (bottom) indicate that the A2bp1 signal is primarily nuclear. Scale bar, 10 μm.

See also Figure S3 and Tables S1 and S2.

Eighteen of the lines tested had potential memory functions (Table S2). These lines, along with two additional lines that failed to produce progeny with *nSyb-GAL4*, were further tested with the MBn driver *R13F02-GAL4*. This two-step screening strategy, first with a pan-neuronal GAL4 driver followed by a MBn-specific GAL4 driver, identified three RNAi lines that produced a memory phenotype with MB expression (Figure 4A). The three candidates include *A2bp1*, a gene encoding a known RNA binding protein involved in alternative splicing (Lee et al., 2009; Fogel et al., 2012); *CG3630*, a gene encoding a protein containing a Costars domain but with a previously unknown biological function (http://flybase.org); and *Cp38*, a gene encoding a chorion protein necessary for eggshell formation (Spradling et al., 1980). Among the three candidate genes, *A2bp1* was the strongest candidate due to its three predicted *miR-980* binding sites in its 3′ UTR (Figure 4B). Furthermore, logic offered *A2bp1* as the most likely choice among the three with a possible authentic role in the biology of memory formation. Memory impairment in *A2bp1 RNAi* in MBs was not due to defects in odor and shock perception (Figure S3C). We thus focused on *A2bp1* as potential target for *miR-980*-based memory phenotypes.

A2bp1 Is Expressed in the Nuclei of Most Brain Neurons

Immunostaining of the *Drosophila* brain with an A2bp1 antisera (Tastan et al., 2010) showed that A2bp1 is expressed broadly in the fly brain (Figure 4C). We marked the cell membranes by expressing mCD8::GFP (Lee and Luo, 1999) and labeled the brains with anti-GFP, anti-A2bp1, and DAPI. High-magnification images showed that the *A2bp1* and *GFP* signals were distinct from one another, and that the *A2bp1* signal overlapped with DAPI staining. This nuclear localization of *Drosophila A2bp1* is consistent with a role for the protein in alternative splicing as demonstrated for other organisms (Jin et al., 2003; Nakahata and Kawamoto, 2005; Underwood et al., 2005; Fogel et al., 2012).

MiR-980 Represses A2bp1 Protein Expression

We tested the effect of the *A2bp1-RNAi* on A2bp1 expression by immunostaining *nSyb-GAL4>UAS-A2bp1 RNAi;UAS-dcr-2* brains (Figure 5A) and quantifying the mean signal intensity from the central brain compared to control brains. We measured an ~50% reduction in signal from RNAi knockdown brains compared to the no-RNAi control (Figure 5A). We confirmed this estimate using western blotting of adult heads with the same antibody (Tastan et al., 2010), identifying a protein exhibiting strong immunoreactivity with an apparent mass of ~105 kDa (Figure S3A). The western blot signal from the ~105 kDa A2bp1 protein in RNAi knockdown flies was reduced by ~50%

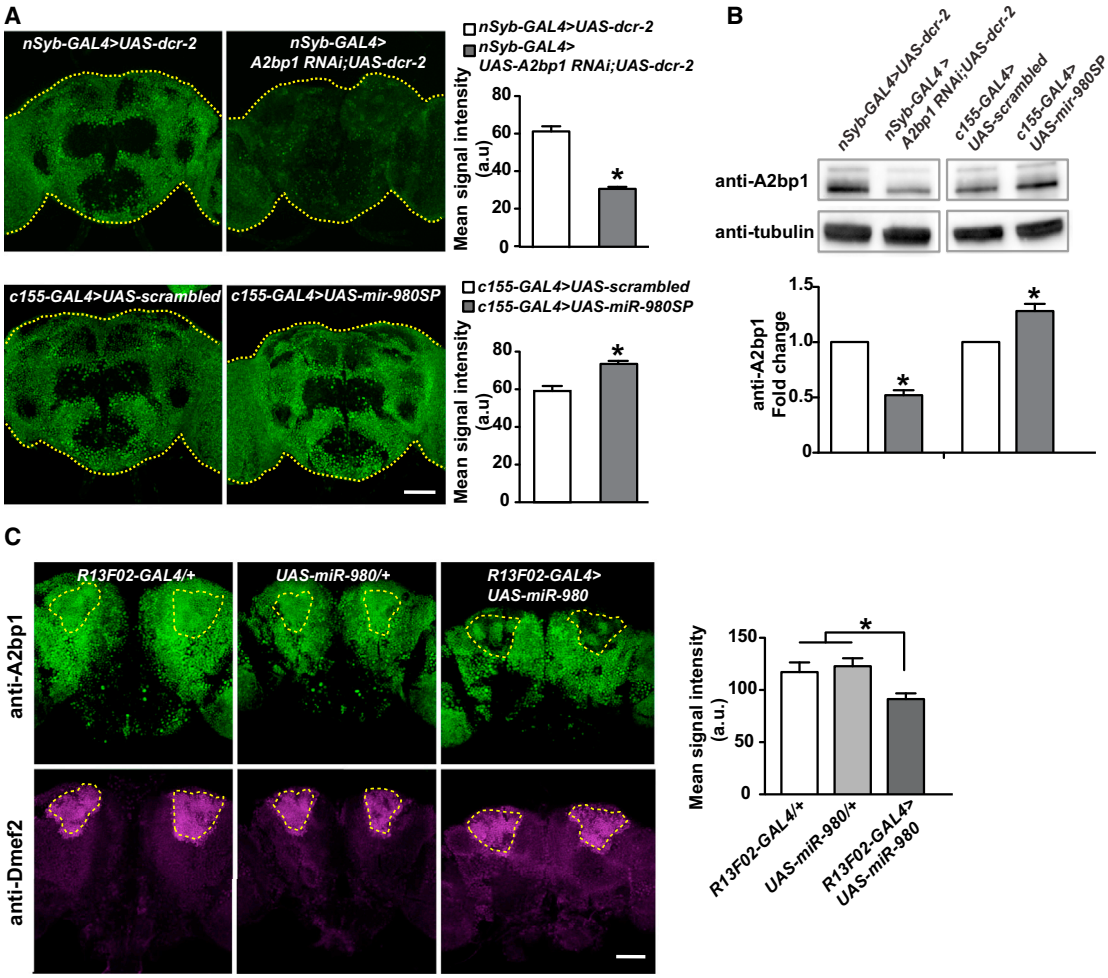

Figure 5. *MiR-980* Inhibits *A2bp1* Expression by Associating with *A2bp1* mRNA

(A) Maximum projection images of the central brain from *nSyb-GAL4>UAS-dcr-2* and *nSyb-GAL4>UAS-A2bp1-RNAi;UAS-dcr-2* flies (top row); and *c155-GAL4>scrambled* and *c155-GAL4>miR-980SP* flies (bottom row) stained with anti-A2bp1 antisera. Each brain is outlined with a yellow dotted line. The mean signal intensity from the central brain is quantified in the adjacent histogram. Expression of the *A2bp1-RNAi* reduced the signal by ~50% compared to the no-RNAi control ($n \geq 11$, $p < 0.0001$). Expression of *miR-980SP* increased the signal by ~25% compared to the *scrambled* control ($n \geq 20$, $p < 0.0001$). Statistics: data were analyzed by two-tailed, two-sample Student's t tests. Scale bar, 50 μm. Results are the mean ± SEM.

(B) Representative anti-A2bp1 and anti-α-tubulin western blots using: (1) *nSyb-GAL4>UAS-dcr-2*, (2) *nSyb-GAL4>UAS-A2bp1-RNAi;UAS-dcr-2* (3), *c155-GAL4>scrambled*, and (4) *c155-GAL4>miR-980SP* fly heads. The signal from the *A2bp1* band was first normalized to the α-tubulin signal in its own lane, and then the control samples were then normalized to 1.0 to calculate the fold change in the experimental groups. *A2bp1-RNAi* expression reduced protein levels by ~50% compared to the no-RNAi control. Expression of *miR-980SP* increased A2bp1 by ~25% compared to the *scrambled* control. Statistics: data were analyzed by one-sample Student's t test. Results are the mean ± SEM with n = 8. $p < 0.0001$ for *A2bp1* RNAi and $p < 0.01$ for *miR-980SP*.

(C) Overexpression of *miR-980* in MB represses A2bp1 expression. Single section images of the central brain stained with anti-A2bp1 (green) and anti-Dmef2 (magenta) antibodies. *R13F02-GAL4/+* and *UAS-miR-980/+* brains were used as controls for the *R13F02-GAL4>UAS-miR-980* genotype. MBn as defined by *Dmef2* immunoreactivity are outlined with yellow dotted lines and mean signal intensity for the region of interest was measured. Overexpressing *miR-980* in MBn decreased the anti-*A2bp1* ~25%. Statistics: the data were analyzed by one-way ANOVA followed by Bonferroni's post hoc tests. Results are the mean ± SEM with n = 15–17. $p < 0.01$. Scale bar, 50 μm.

See also Figure S3.

compared to control flies (Figures 5B and S4A). The western blots resolved a less abundant isoform of ~125 kDa that also responded to *A2bp1 RNAi* expression. The significant decrease in A2bp1 protein upon RNAi knockdown provides molecular support for the effect of the *A2bp1* RNAi on behavior (Figure 4A). Using the same antibody, we tested whether expression of *A2bp1* is altered when *miR-980SP* is expressed. Inhibiting *miR-980* with *miR-980SP* expression using the pan-neuronal *c155-GAL4* driver significantly increased A2bp1 protein by ~25% as detected by both immunostaining (Figure 5A) and western blotting (Figures 5B and S4A).

We also tested the effect of *miR-980* overexpression on *A2bp1* protein level. *MiR-980* overexpression using the pan-neuronal *c155-GAL4* driver produced pupal lethality. Therefore, we tested

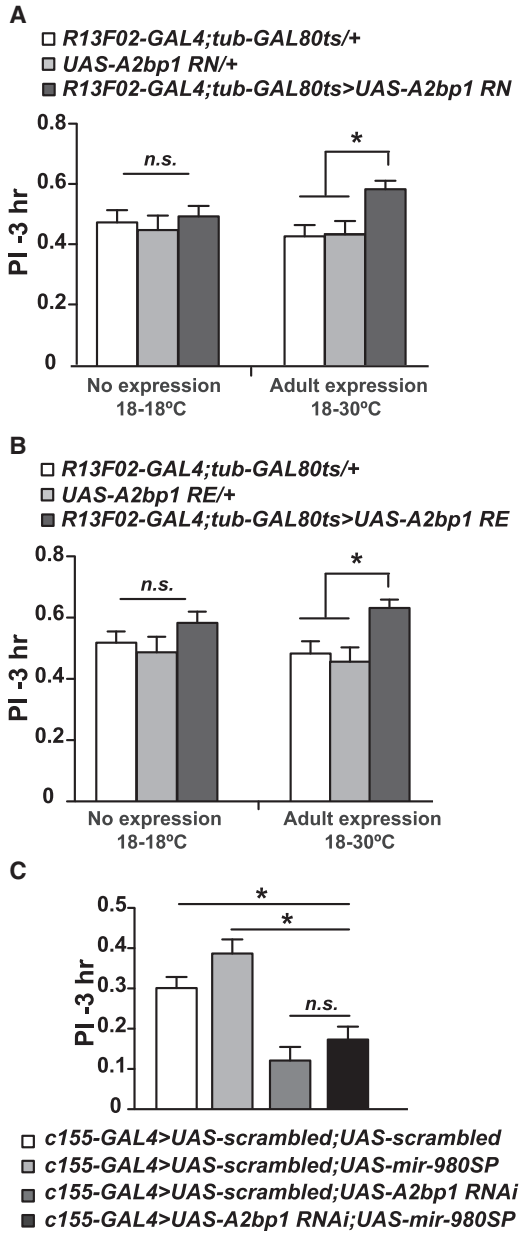

Figure 6. Overexpression of A2bp1 Potentiates Memory; Decreasing A2bp1 Reverses the Memory Enhancement Due to *miR-980SP* Expression

(A) Adult-specific overexpression of the *A2bp1RN* isoform increases 3 hr memory. MB-specific expression of *UAS-A2bp1RN* was driven by *R13F02-GAL4* in the presence of Gal80^{ts} to restrict transgene expression to adulthood. Flies were kept at 18°C throughout development and adulthood (left) or at 18°C during development and switched to 30°C after hatching (right) to induce *UAS-A2bp1* overexpression. A2bp1 overexpression in the MB significantly improved memory compared to UAS-only and GAL4-only controls. Statistics: PIs were analyzed using one-way ANOVA followed by Bonferroni's post hoc tests. PIs are the mean ± SEM with n = 20. $p < 0.01$.

(B) Adult-specific overexpression of the A2bp1RE isoform increases 3 hr memory. MB-specific expression of a second A2bp1 isoform, *UAS-A2bp1(RE)*, during adulthood also enhanced 3 hr memory. Statistics: PIs were analyzed using one-way ANOVA followed by Bonferroni's post hoc tests. PIs are the mean ± SEM with n = 15. $p < 0.01$.

(C) *A2bp1* is genetically downstream of *miR-980*. The *UAS-A2bp1 RNAi* and *UAS-miR-980SP* transgenes were combined with a *UAS-scrambled* transgene in order to obtain flies with the same number of *UAS*-elements as in the *UAS-A2bp1 RNAi;UAS-miR-980SP* experimental group. The *UAS-scrambled* transgenes inserted at the *attP40* and *attP2 sites* were combined together and used as the control. Expression was driven by *c155-GAL4*. Three-hour PIs of *UAS-A2bp1 RNAi;UAS-miR-980 SP* expressing flies were significantly lower than the *scrambled* control and *miR-980SP*-expressing flies, but not significantly different from *A2bp1 RNAi*-expressing flies. Statistics: scores were analyzed using one-way ANOVA followed by Bonferroni's post hoc tests. PIs are the mean ± SEM with n = 36 for the double *scrambled* control and n = 21 for all other groups. $p < 0.0001$.

See also Figures S3 and S4.

the effects of overexpression using the MBn-specific driver *R13F02-GAL4* and identified the cell bodies of MBn with Dmef2 co-labeling (Figure 5C). We measured the anti-*A2bp1* mean signal intensity in the MBn for *R13F02-GAL4>UAS-miR-980*, UAS-only, and GAL4-only genotypes. Opposite to the results obtained with *miR-980* inhibition, elevating *miR-980* in MBn significantly decreased *A2bp1* expression by ~25% (Figure 5C). These results show that *miR-980* represses the expression of the A2bp1 protein.

Overexpression of *A2bp1* in the Adult Mushroom Bodies Enhances Memory

The current annotation of the *A2bp1* gene predicts eight different protein isoforms, ranging in size from 547 to 962 amino acids, produced by eight RNAs due to transcription from two transcriptional start sites and alternative splicing (http://flybase.org). It is unknown which of the isoforms dominate expression in the adult head. We designed primers to amplify RNA transcripts from the largest transcriptional unit by PCR using head cDNA and recovered six new splice variants, none of which corresponded to the largest previously annotated isoforms, RH and RL (Figure S3B). We picked one of the two most abundant splice variants and generated *UAS-A2bp1* overexpression flies that lack *miR-980* binding 3′ UTR sites in the transgene. We named the new splice variant RN. It differs from the annotated form, RH, only by the exclusion of exon 6.

If an increased expression of *A2bp1* is the primary reason for the enhanced memory observed in *miR-980*-inhibited flies due to inadequate repression by *miR-980*, then overexpressing *UAS-A2bp1* should enhance memory. Driving *UAS-A2bp1RN* with *R13F02-GAL4* resulted in embryonic lethality due to unknown developmental defects. We therefore tested whether overexpression, limited to the MB during adulthood, would enhance memory. Restricting *A2bp1* expression in adult MB using *R13F02-GAL4;tub-GAL80^{ts}* resulted in an ~3- to 4-fold increase in A2bp1 abundance measured by western blotting and immunohistochemistry (Figures S4B and S4C). Importantly, *A2bp1* overexpression in the adult MB without the constraints imposed by *miR-980* repression mimicked the effects of *miR-980* inhibition, with a significant memory improvement measured at 3 hr compared to *UAS*-only and *GAL4*-only controls without altering odor and shock perception (Figures 6A and S3D). We also tested a second *A2bp1* isoform, *RE* in adults (Usha and Shashidhara, 2010), and observed the same memory enhancement (Figures 6B and S3D). These results support the model that enhanced

memory occurring from *miR-980* inhibition results predominantly from the dysregulation in the MBn of the *miR-980* target, *A2bp1* mRNA. Since overexpression of both isoforms of *A2bp1* produced the same memory enhancement, the results also reveal that exons 2, 11, and 13 are unimportant for this function.

MicroRNAs as regulators of mRNA expression are, in essence, upstream of the mRNA targets in the molecular signaling within a cell. To test the predicted genetic interaction between *miR-980* and *A2bp1*, we performed an epistasis experiment combining in the same fly the expression of *UAS-miR-980SP* that promotes memory, with the expression of the *UAS-A2bp1 RNAi* transgene that inhibits memory. We compared the memory scores of this experimental group to *UAS-A2bp1 RNAi* or *UAS-miR-980SP* controls. The *A2bp1 RNAi;miR-980SP* double transgenic flies had memory scores significantly lower than both *miR-980SP* and scrambled controls, indicating that *miR-980SP* expression loses its normal memory enhancing effect when *A2bp1* is reduced (Figure 6C). In addition, the memory scores of the *A2bp1 RNAi; miR-980SP* double transgenic flies were not different statistically from those of flies expressing *A2bp1 RNAi* alone. Thus, the observed change in A2bp1 protein abundance by altering *miR-980* levels, the improvement of memory with *miR-980* inhibition and A2bp1 overexpression, and results from epistasis experiments are consistent with the model that the normal memory suppressing effects of *miR-980* occur through its regulation of the memory-promoting gene, A2bp1.

DISCUSSION

MicroRNAs are highly expressed in the vertebrate and invertebrate brain and contribute to fine-tuning of gene expression during development and during physiological events in cells. Nevertheless, their functional roles in the neuronal plasticity underlying learning and memory remains largely unexplored. We previously conducted a behaviorally based "miRNA sponge screen" to systematically identify the miRNAs involved in *Drosophila* olfactory aversive learning and memory (Busto et al., 2015). The results presented here offer five major advances in our knowledge about the function of this class of regulatory molecules: (1) *miR-980* functions to suppress memory formation by acting in multiple types of neurons within the olfactory nervous system; (2) *miR-980* works as a suppressor of acquisition and memory stability; (3) *miR-980* suppresses the excitability of excitatory neurons; (4) the memory suppressor functions of *miRNA-980* are mediated largely by the inhibition of the autism-susceptibility gene, *A2bp1*; and (5) *A2bp1*, itself, is a memory-promoting gene.

One surprising observation made in our study was that inhibition of *miR-980* in multiple neurons within the olfactory nervous system enhances memory performance, as we anticipated finding a single cellular focus for its effects. Initially, it was difficult to understand how a single microRNA could modify behavioral memory when altered in one of many different types of neurons. This was reconciled by showing that excitability of Pns is enhanced with inhibited *miR-980* function, offering the explanation that increased signaling, in general, within the olfactory nervous system enhances behavioral memory. This model provides a general explanation for the effects of *miR-980* that function in multiple classes of excitable neurons.

We propose that the role of *miR-980* in excitability accounts for the increased acquisition when the *miRNA* is inhibited. An increase in excitable state may simply enhance the signaling through different neuron types within the olfactory nervous system as the organism integrates sensory information into memory. A corollary of this idea is that normal acquisition is a composite effect of multiple neurons within the circuit conveying the sensory information being learned. Although it is possible that increased acquisition also accounts for the increased memory performance observed when immediate performance scores were normalized, an alternative possibility is that *miR-980* may have distinct roles in acquisition and memory stability. For instance, although we attribute the increased acquisition to increased neuronal excitability, the increased memory after acquisition may be due to altered regulation of molecules involved in synaptic transmission.

MiR-980 belongs to the *miR-22* family of miRNAs found in mammals (Ruby et al., 2007). Within the nervous system, the *miR-22* family has been reported to participate in neuroprotection (Yu et al., 2015; Jovicic et al., 2013), neurodegeneration (Lee et al., 2011), neuroinflammation (Parisi et al., 2013; Siegel et al., 2012), neurodevelopment (Volvert et al., 2014; Berenguer et al., 2013), and neuroplasticity (Chen et al., 2013). Thus, although this family appears to have multiple roles in the nervous system and disease, our current studies identify members of this family as specifically involved in the suppression of memory formation. Given the functional association between *miR-980* and *A2bp1* shown here, it is also tempting to speculate that the *miR-980/miR-22* family of *miRNAs* might be associated with ASD. No evidence for this possibility has yet been reported, but the expression of *miR-22* is reduced in attention deficit hyperactivity disorder (ADHD) (Kandemir et al., 2014) and is genetically associated with panic disorder and anxiety in humans (Muiños-Gimeno et al., 2011). Thus, there are neuropsychiatric links to *miR-22*, which could potentially be through a role in excitability. Moreover, *miR-22* represses the tumor suppressor gene *PTEN* in transformed human bronchial epithelial cells (Liu et al., 2010), and *PTEN* is known to be involved in Cowden syndrome and ASD in humans (Goffin et al., 2001).

Our behavioral, molecular, cellular, and genetic data together argue that *A2bp1* is a primary target of *miR-980* for memory suppression. First, A2bp1 is broadly expressed in the fly brain, consistent with a broad nervous system requirement for *miR-980*. Second, there are three *miR-980* binding sites in *A2bp1* 3′ UTR making it a strong candidate mRNA target for *miR-980* regulation. Third, we performed an in vitro mRNA binding experiment using biotinylated mature *miR-980* as bait and successfully captured eight times more *A2bp1* mRNA using wild-type *miR-980* versus a form mutated for the seed region (data not shown). Fourth, A2bp1 shows the precise abundance/behavior relationship predicted as a direct target of *miR-980*. Overexpression of A2bp1 increases memory; *miR-980* suppression increases memory. *A2bp1* knockdown impairs memory; *miR-980* overexpression impairs memory. Fifth, A2bp1 protein abundance varies as expected by manipulation of *miR-980* levels. Overexpression of *miR-980* decreases A2bp1 protein abundance and *miR-980* suppression increases A2bp1 protein abundance. Finally, reducing *A2bp1* levels using RNAi in

miR-980-inhibited flies reversed the memory improvement. This finding is consistent with the model that *A2bp1* is genetically downstream of *miR-980* and a major mediator of the phenotype. However, we cannot exclude the possibilities that there may be additional *miR-980* targets that participate in memory suppression and *miR-980* regulation of *A2bp1* could be indirect. Our simple model for *miR-980/A2bp1* interactions and function seem to be at odds with an observation made about *A2bp1* using mammalian models. In the mouse (Gehman et al., 2011), neuronal-specific knockout of *A2bp1* increases excitability in the dentate gyrus, a result opposite of that predicted by our model. This difference might reflect species or cell type differences, the complexity of the gene with its dozens of isoforms, or the multiple layers of regulation on *A2bp1* expression. Bioinformatics analyses predict multiple *miRNAs* as binding to the *A2bp1* 3′ UTR and regulating its expression. Thus, its basal or regulated expression level due to changes in physiological state could be a composite of many different regulatory molecules.

A2bp1 is associated with autism and epilepsy in human patients (Bhalla et al., 2004; Martin et al., 2007; Sebat et al., 2007; Mikhail et al., 2011; Davis et al., 2012) functioning presumably by regulating alternative splicing during both development and in adults (Lee et al., 2009; Fogel et al., 2012). Corominas et al. (2014) proposed that changes in gene-splicing alter the relative abundance of protein isoforms, which remodels protein networks and increases the risk for autism. Consistent with this thought, transcriptome analyses from ASD brains identified *A2bp1* as one hub gene that is dysregulated in patients with autism (Voineagu et al., 2011). *A2bp1* was originally identified through its interaction with Ataxin-2 (Shibata et al., 2000). Pn-specific knockdown of *Ataxin-2* impairs long-term olfactory habituation-associated structural and functional plasticity by regulating the miRNA pathway (McCann et al., 2011). Future studies will shed light on whether memory phenotypes of *A2bp1* are dependent on *Ataxin-2.*

It is intriguing that our studies show that adult stage-specific increases in *A2bp1* abundance improve aversive olfactory memory, independent of any developmental function for the protein, and human ASD is a spectrum brain disorder that is associated with poor to extraordinarily robust learning and memory capacities (Grzadzinski et al., 2013). We speculate that the different protein interaction networks that form due to varying levels of *A2bp1* function account for the range of intellectual abilities observed in ASD. *Drosophila* may prove to be a much speedier and simpler system to dissect the specific effect of *A2bp1* abundance on the emergence of protein interaction networks and their influence on cognitive abilities.

EXPERIMENTAL PROCEDURES

Fly Stocks and Behavior

Flies were cultured using standard methods. One- to 4-day-old flies were used for the behavioral experiments. Approximately 30 min before training, flies were transferred and maintained in the behavior room (dim red light, 25°C, ~70% humidity). For conditioning, ~50–60 flies were trained using a standard two-odor discriminative aversive conditioning paradigm (Berry et al., 2012) by exposing flies to 1 min of CS+ odor paired with 12 electric shock pulses followed by 30 s of air and 1 min of the CS− odor. Memory was tested using a T-maze, which delivers CS+ from one arm and CS− from the other. Additional details about the fly stocks utilized in this study and behavioral tests are provided in the Supplemental Experimental Procedures.

In Vivo Ca^{2+} Imaging

Flies were mounted onto recording chamber as described previously (Berry et al., 2012). Briefly, a single fly was aspirated, without anesthesia, into a custom-designed recording chamber. The head was immobilized by gluing the eyes to the chamber with myristic acid and the proboscis similarly immobilized. A small area of dorsal cuticle was removed to provide optical access to the brain. Fresh saline (103 mM NaCl, 3 mM KCl, 5 mM HEPES, 1.5 mM $CaCl_2$, 4 mM $MgCl_2$, 26 mM $NaHCO_3$, 1 mM NaH_2PO_4, 10 mM trehalose, 7 mM sucrose, and 10 mM glucose [pH 7.2]) was perfused across the brain to prevent desiccation and ensure the health of the fly. We recorded the responses in MB using a 25× water-immersion objective. Odorants were diluted 1:10 in mineral oil and spread on a 1 cm^2 filter paper in a scintillation vial. Pressurized air was passed through the vial to deliver a 3-s pulse of air laced with oct vapor at a rate of 200 ml/min, followed 3 min later by a second pulse of air laced with ben vapor. Images were acquired at 4 frames/s at a resolution of 256 × 256 pixels from both MB vertical and horizontal lobes. The image data were analyzed as described previously (Yu et al., 2005; Cervantes-Sandoval et al., 2013). For statistical analysis, $\Delta F/F_o$ responses from vertical and horizontal lobes were normalized to the scramble control. Significance was determined using one-way ANOVA followed by Bonferroni's post hoc tests.

Whole Cell Recordings from Projection Neurons in Isolated Adult Brain

Brains were obtained from adult female flies 2 days after eclosion. The entire brain was removed from the head and mounted in the recording chamber with the anterior face of the brain up (Gu and O'Dowd, 2006, 2007). Recordings were made from projection neurons (Pn) in the dorsal neuron cluster using 8–9 MΩ resistance pipettes. All voltages reported refer to pipette potentials at the soma. Depolarization-evoked action potentials were recorded using a pipette solution containing (in mM) 102 potassium gluconate, 0.085 $CaCl_2$, 1.7 $MgCl_2$, 17 NaCl, 0.94 EGTA, 8.5 HEPES, and 4.5 ATP. The pH was adjusted to 7.2 and osmolarity to 234–236 mOsM. The chamber was continuously perfused at 0.5 ml/min with recording solution that contained (in mM) 120 NaCl, 1.8 $CaCl_2$, 0.8 $MgCl_2$, 3 KCl, 5 glucose, 10 HEPES, as well as the synaptic receptor blockers D-turbocurarine (20 μM) and picrotoxin (10 μM). The pH was adjusted to 7.2 and osmolarity to 250–253 mOsM. Data shown were corrected for the 5 mV liquid junction potential generated in these solutions. For examination of the evoked firing properties, the membrane potential was held at −65 mV by injection of hyperpolarizing holding current. Data were acquired with a Patch Clamp L/M-EPC7 amplifier (List Medical), a digidata 1322A D-A converter (Molecular Devices), a Dell computer (Dimension 8200), and pClamp9 software (Molecular Devices).

Bioinformatics and Statistical Analyses

Putative mRNA targets for *miR-980* were predicted using online tools TargetScan (http://Targetscan.org) and microRNA.org (http://microRNA.org). TargetScan predicts 70 mRNA targets for *miR-980.* We identified 25 additional and non-overlapping candidates from microRNA.org (Enright et al., 2003; Kheradpour et al., 2007; Ruby et al., 2007). Prism was used for statistical analyses. Two sample, two-tailed Student's t tests were used to compare two conditions. To compare one group to a normalized control group, a one sample, two-tailed, Student's t test was used. For multiple group comparisons, one-way ANOVA followed by Bonferroni's post hoc tests were used.

Immunohistochemistry

Two- to 5-day-old female fly brains were dissected in 1× PBS and transferred to 1% paraformaldehyde in PBS. We followed the protocol described by Fly Light Project (Jenett et al., 2012). Additional details are found in the Supplemental Experimental Procedures.

ACCESSION NUMBERS

The accession number for the A2bp1RN (cDNA sequence) reported in this paper is GenBank: KU315475.

SUPPLEMENTAL INFORMATION

Supplemental Information includes Supplemental Experimental Procedures, four figures, and two tables and can be found with this article online at http://dx.doi.org/10.1016/j.celrep.2016.01.040.

AUTHOR CONTRIBUTIONS

T.G., G.U.B., and R.L.D. designed the behavioral, immunohistochemical, and biochemical experiments. T.G. performed these experiments. T.G. and I.C. designed and performed the imaging experiments. S.S.S. and D.K.O. designed and performed the whole cell patch clamp recordings. T.G. and R.L.D. wrote the initial draft of the manuscript that was then edited by all authors.

ACKNOWLEDGMENTS

We would like to acknowledge David Van Vactor (Harvard) and Tudor Fulga (Oxford) for the *miRNA* sponge lines. We thank Eric Lai (Sloan Kettering), L.S. Shashidhara (Indian Institute of Science Education and Research), Stephen Cohen (University of Copenhagen), the Kyoto *Drosophila* Genetic Resource Center, and the Vienna Drosophila RNAi center (VDRC) for RNAi and other fly lines. We are grateful to Michael Buszczak (UT Southwestern) for the anti-A2bp1 antisera, Eric Olson (UT Southwestern) for the anti-Dmef2 antibody, Courtney M. MacMullen and Molee Chakraborty for technical support, and Neelam Shahani for help in obtaining high-magnification images. This research was supported by NIH R37 NS19904 and R01 NS052351 to R.L.D. and NIH RO1 NS0830009 to D.K.O.

Received: July 8, 2015
Revised: October 26, 2015
Accepted: January 9, 2016
Published: February 11, 2016

REFERENCES

Ambros, V. (2004). The functions of animal microRNAs. Nature *431*, 350–355.

Ashraf, S.I., McLoon, A.L., Sclarsic, S.M., and Kunes, S. (2006). Synaptic protein synthesis associated with memory is regulated by the RISC pathway in *Drosophila*. Cell *124*, 191–205.

Bartel, D.P. (2009). MicroRNAs: target recognition and regulatory functions. Cell *136*, 215–233.

Bartel, D.P., and Chen, C.Z. (2004). Micromanagers of gene expression: the potentially widespread influence of metazoan microRNAs. Nat. Rev. Genet. *5*, 396–400.

Bejarano, F., Bortolamiol-Becet, D., Dai, Q., Sun, K., Saj, A., Chou, Y.T., Raleigh, D.R., Kim, K., Ni, J.Q., Duan, H., et al. (2012). A genome-wide transgenic resource for conditional expression of *Drosophila* microRNAs. Development *139*, 2821–2831.

Berenguer, J., Herrera, A., Vuolo, L., Torroba, B., Llorens, F., Sumoy, L., and Pons, S. (2013). MicroRNA 22 regulates cell cycle length in cerebellar granular neuron precursors. Mol. Cell. Biol. *33*, 2706–2717.

Berry, J.A., Cervantes-Sandoval, I., Nicholas, E.P., and Davis, R.L. (2012). Dopamine is required for learning and forgetting in *Drosophila*. Neuron *74*, 530–542.

Bhalla, K., Phillips, H.A., Crawford, J., McKenzie, O.L., Mulley, J.C., Eyre, H., Gardner, A.E., Kremmidiotis, G., and Callen, D.F. (2004). The de novo chromosome 16 translocations of two patients with abnormal phenotypes (mental retardation and epilepsy) disrupt the A2BP1 gene. J. Hum. Genet. *49*, 308–311.

Bredy, T.W., Lin, Q., Wei, W., Baker-Andresen, D., and Mattick, J.S. (2011). MicroRNA regulation of neural plasticity and memory. Neurobiol. Learn. Mem. *96*, 89–94.

Busto, G.U., Guven-Ozkan, T., Fulga, T.A., Van Vactor, D., and Davis, R.L. (2015). MicroRNAs that promote or inhibit memory formation in *Drosophila melanogaster*. Genetics *200*, 569–580.

Cervantes-Sandoval, I., Martin-Peña, A., Berry, J.A., and Davis, R.L. (2013). System-like consolidation of olfactory memories in *Drosophila*. J. Neurosci. *33*, 9846–9854.

Chen, C.L., Liu, H., and Guan, X. (2013). Changes in microRNA expression profile in hippocampus during the acquisition and extinction of cocaine-induced conditioned place preference in rats. J. Biomed. Sci. *20*, 96.

Corominas, R., Yang, X., Lin, G.N., Kang, S., Shen, Y., Ghamsari, L., Broly, M., Rodriguez, M., Tam, S., Trigg, S.A., et al. (2014). Protein interaction network of alternatively spliced isoforms from brain links genetic risk factors for autism. Nat. Commun. *5*, 3650.

Davis, R.L. (2005). Olfactory memory formation in *Drosophila*: from molecular to systems neuroscience. Annu. Rev. Neurosci. *28*, 275–302.

Davis, R.L. (2011). Traces of *Drosophila* memory. Neuron *70*, 8–19.

Davis, L.K., Maltman, N., Mosconi, M.W., Macmillan, C., Schmitt, L., Moore, K., Francis, S.M., Jacob, S., Sweeney, J.A., and Cook, E.H. (2012). Rare inherited A2BP1 deletion in a proband with autism and developmental hemiparesis. Am. J. Med. Genet. A. *158A*, 1654–1661.

Dietzl, G., Chen, D., Schnorrer, F., Su, K.C., Barinova, Y., Fellner, M., Gasser, B., Kinsey, K., Oppel, S., Scheiblauer, S., et al. (2007). A genome-wide transgenic RNAi library for conditional gene inactivation in *Drosophila*. Nature *448*, 151–156.

Ebert, M.S., Neilson, J.R., and Sharp, P.A. (2007). MicroRNA sponges: competitive inhibitors of small RNAs in mammalian cells. Nat. Methods *4*, 721–726.

Enright, A.J., John, B., Gaul, U., Tuschl, T., Sander, C., and Marks, D.S. (2003). MicroRNA targets in *Drosophila*. Genome Biol. *5*, R1.

Fogel, B.L., Wexler, E., Wahnich, A., Friedrich, T., Vijayendran, C., Gao, F., Parikshak, N., Konopka, G., and Geschwind, D.H. (2012). RBFOX1 regulates both splicing and transcriptional networks in human neuronal development. Hum. Mol. Genet. *21*, 4171–4186.

Fulga, T.A., McNeill, E.M., Binari, R., Yelick, J., Blanche, A., Booker, M., Steinkraus, B.R., Schnall-Levin, M., Zhao, Y., DeLuca, T., et al. (2015). A transgenic resource for conditional competitive inhibition of conserved *Drosophila* microRNAs. Nat. Commun. *6*, 7279.

Gehman, L.T., Stoilov, P., Maguire, J., Damianov, A., Lin, C.H., Shiue, L., Ares, M., Jr., Mody, I., and Black, D.L. (2011). The splicing regulator Rbfox1 (A2BP1) controls neuronal excitation in the mammalian brain. Nat. Genet. *43*, 706–711.

Goffin, A., Hoefsloot, L.H., Bosgoed, E., Swillen, A., and Fryns, J.P. (2001). PTEN mutation in a family with Cowden syndrome and autism. Am. J. Med. Genet. *105*, 521–524.

Grzadzinski, R., Huerta, M., and Lord, C. (2013). DSM-5 and autism spectrum disorders (ASDs): an opportunity for identifying ASD subtypes. Mol. Autism *4*, 12.

Gu, H., and O'Dowd, D.K. (2006). Cholinergic synaptic transmission in adult *Drosophila* Kenyon cells in situ. J. Neurosci. *26*, 265–272.

Gu, H., and O'Dowd, D.K. (2007). Whole cell recordings from brain of adult Drosophila. J. Vis. Exp. *6*, 248.

Guven-Ozkan, T., and Davis, R.L. (2014). Functional neuroanatomy of *Drosophila* olfactory memory formation. Learn. Mem. *21*, 519–526.

Iniguez, J., Schutte, S.S., and O'Dowd, D.K. (2013). Cav3-type α1T calcium channels mediate transient calcium currents that regulate repetitive firing in Drosophila antennal lobe PNs. J. Neurophysiol. *110*, 1490–1496.

Jenett, A., Rubin, G.M., Ngo, T.T., Shepherd, D., Murphy, C., Dionne, H., Pfeiffer, B.D., Cavallaro, A., Hall, D., Jeter, J., et al. (2012). A GAL4-driver line resource for *Drosophila* neurobiology. Cell Rep. *2*, 991–1001.

Jin, Y., Suzuki, H., Maegawa, S., Endo, H., Sugano, S., Hashimoto, K., Yasuda, K., and Inoue, K. (2003). A vertebrate RNA-binding protein Fox-1 regulates tissue-specific splicing via the pentanucleotide GCAUG. EMBO J. *22*, 905–912.

Jovicic, A., Zaldivar Jolissaint, J.F., Moser, R., Silva Santos, Mde.F., and Luthi-Carter, R. (2013). MicroRNA-22 (miR-22) overexpression is neuroprotective via general anti-apoptotic effects and may also target specific Huntington's disease-related mechanisms. PLoS ONE *8*, e54222.

Kandemir, H., Erdal, M.E., Selek, S., Ay, O.I., Karababa, I.F., Kandemir, S.B., Ay, M.E., Yılmaz, S.G., Bayazıt, H., and Taşdelen, B. (2014). Evaluation of several micro RNA (miRNA) levels in children and adolescents with attention deficit hyperactivity disorder. Neurosci. Lett. *580*, 158–162.

Kheradpour, P., Stark, A., Roy, S., and Kellis, M. (2007). Reliable prediction of regulator targets using 12 *Drosophila* genomes. Genome Res. *17*, 1919–1931.

Konopka, W., Kiryk, A., Novak, M., Herwerth, M., Parkitna, J.R., Wawrzyniak, M., Kowarsch, A., Michaluk, P., Dzwonek, J., Arnsperger, T., et al. (2010). MicroRNA loss enhances learning and memory in mice. J. Neurosci. *30*, 14835–14842.

Kosik, K.S. (2006). The neuronal microRNA system. Nat. Rev. Neurosci. *7*, 911–920.

Lee, T., and Luo, L. (1999). Mosaic analysis with a repressible cell marker for studies of gene function in neuronal morphogenesis. Neuron *22*, 451–461.

Lee, R.C., Feinbaum, R.L., and Ambros, V. (1993). The *C. elegans* heterochronic gene lin-4 encodes small RNAs with antisense complementarity to lin-14. Cell *75*, 843–854.

Lee, J.A., Tang, Z.Z., and Black, D.L. (2009). An inducible change in Fox-1/A2BP1 splicing modulates the alternative splicing of downstream neuronal target exons. Genes Dev. *23*, 2284–2293.

Lee, S.T., Chu, K., Im, W.S., Yoon, H.J., Im, J.Y., Park, J.E., Park, K.H., Jung, K.H., Lee, S.K., Kim, M., and Roh, J.K. (2011). Altered microRNA regulation in Huntington's disease models. Exp. Neurol. *227*, 172–179.

Li, W., Cressy, M., Qin, H., Fulga, T., Van Vactor, D., and Dubnau, J. (2013). MicroRNA-276a functions in ellipsoid body and mushroom body neurons for naive and conditioned olfactory avoidance in *Drosophila*. J. Neurosci. *33*, 5821–5833.

Liu, L., Jiang, Y., Zhang, H., Greenlee, A.R., Yu, R., and Yang, Q. (2010). miR-22 functions as a micro-oncogene in transformed human bronchial epithelial cells induced by anti-benzo[a]pyrene-7,8-diol-9,10-epoxide. Toxicol. In Vitro *24*, 1168–1175.

Loya, C.M., Lu, C.S., Van Vactor, D., and Fulga, T.A. (2009). Transgenic microRNA inhibition with spatiotemporal specificity in intact organisms. Nat. Methods *6*, 897–903.

Marrone, A.K., Edeleva, E.V., Kucherenko, M.M., Hsiao, N.H., and Shcherbata, H.R. (2012). Dg-Dys-Syn1 signaling in *Drosophila* regulates the microRNA profile. BMC Cell Biol. *13*, 26.

Martin, C.L., Duvall, J.A., Ilkin, Y., Simon, J.S., Arreaza, M.G., Wilkes, K., Alvarez-Retuerto, A., Whichello, A., Powell, C.M., Rao, K., et al. (2007). Cytogenetic and molecular characterization of A2BP1/FOX1 as a candidate gene for autism. Am. J. Med. Genet. B. Neuropsychiatr. Genet. *144B*, 869–876.

McCann, C., Holohan, E.E., Das, S., Dervan, A., Larkin, A., Lee, J.A., Rodrigues, V., Parker, R., and Ramaswami, M. (2011). The Ataxin-2 protein is required for microRNA function and synapse-specific long-term olfactory habituation. Proc. Natl. Acad. Sci. USA *108*, E655–E662.

McGuire, S.E., Le, P.T., Osborn, A.J., Matsumoto, K., and Davis, R.L. (2003). Spatiotemporal rescue of memory dysfunction in *Drosophila*. Science *302*, 1765–1768.

McNeill, E., and Van Vactor, D. (2012). MicroRNAs shape the neuronal landscape. Neuron *75*, 363–379.

Mikhail, F.M., Lose, E.J., Robin, N.H., Descartes, M.D., Rutledge, K.D., Rutledge, S.L., Korf, B.R., and Carroll, A.J. (2011). Clinically relevant single gene or intragenic deletions encompassing critical neurodevelopmental genes in patients with developmental delay, mental retardation, and/or autism spectrum disorders. Am. J. Med. Genet. A. *155A*, 2386–2396.

Muiños-Gimeno, M., Espinosa-Parrilla, Y., Guidi, M., Kagerbauer, B., Sipilä, T., Maron, E., Pettai, K., Kananen, L., Navinés, R., Martín-Santos, R., et al. (2011). Human microRNAs miR-22, miR-138-2, miR-148a, and miR-488 are associated with panic disorder and regulate several anxiety candidate genes and related pathways. Biol. Psychiatry *69*, 526–533.

Nakahata, S., and Kawamoto, S. (2005). Tissue-dependent isoforms of mammalian Fox-1 homologs are associated with tissue-specific splicing activities. Nucleic Acids Res. *33*, 2078–2089.

Parisi, C., Arisi, I., D'Ambrosi, N., Storti, A.E., Brandi, R., D'Onofrio, M., and Volonté, C. (2013). Dysregulated microRNAs in amyotrophic lateral sclerosis microglia modulate genes linked to neuroinflammation. Cell Death Dis. *4*, e959.

Ruby, J.G., Stark, A., Johnston, W.K., Kellis, M., Bartel, D.P., and Lai, E.C. (2007). Evolution, biogenesis, expression, and target predictions of a substantially expanded set of *Drosophila* microRNAs. Genome Res. *17*, 1850–1864.

Saab, B.J., and Mansuy, I.M. (2014). Neuroepigenetics of memory formation and impairment: the role of microRNAs. Neuropharmacology *80*, 61–69.

Schaefer, A., Im, H.I., Venø, M.T., Fowler, C.D., Min, A., Intrator, A., Kjems, J., Kenny, P.J., O'Carroll, D., and Greengard, P. (2010). Argonaute 2 in dopamine 2 receptor-expressing neurons regulates cocaine addiction. J. Exp. Med. *207*, 1843–1851.

Sebat, J., Lakshmi, B., Malhotra, D., Troge, J., Lese-Martin, C., Walsh, T., Yamrom, B., Yoon, S., Krasnitz, A., Kendall, J., et al. (2007). Strong association of de novo copy number mutations with autism. Science *316*, 445–449.

Shibata, H., Huynh, D.P., and Pulst, S.M. (2000). A novel protein with RNA-binding motifs interacts with ataxin-2. Hum. Mol. Genet. *9*, 1303–1313.

Siegel, S.R., Mackenzie, J., Chaplin, G., Jablonski, N.G., and Griffiths, L. (2012). Circulating microRNAs involved in multiple sclerosis. Mol. Biol. Rep. *39*, 6219–6225.

Spradling, A.C., Digan, M.E., Mahowald, A.P., Scott, M., and Craig, E.A. (1980). Two clusters of genes for major chorion proteins of *Drosophila melanogaster*. Cell *19*, 905–914.

Tastan, O.Y., Maines, J.Z., Li, Y., McKearin, D.M., and Buszczak, M. (2010). *Drosophila* ataxin 2-binding protein 1 marks an intermediate step in the molecular differentiation of female germline cysts. Development *137*, 3167–3176.

Turner, G.C., Bazhenov, M., and Laurent, G. (2008). Olfactory representations by *Drosophila* mushroom body neurons. J. Neurophysiol. *99*, 734–746.

Underwood, J.G., Boutz, P.L., Dougherty, J.D., Stoilov, P., and Black, D.L. (2005). Homologues of the *Caenorhabditis elegans* Fox-1 protein are neuronal splicing regulators in mammals. Mol. Cell. Biol. *25*, 10005–10016.

Usha, N., and Shashidhara, L.S. (2010). Interaction between Ataxin-2 binding protein 1 and Cubitus-interruptus during wing development in *Drosophila*. Dev. Biol. *341*, 389–399.

Voineagu, I., Wang, X., Johnston, P., Lowe, J.K., Tian, Y., Horvath, S., Mill, J., Cantor, R.M., Blencowe, B.J., and Geschwind, D.H. (2011). Transcriptomic analysis of autistic brain reveals convergent molecular pathology. Nature *474*, 380–384.

Volvert, M.L., Prévot, P.P., Close, P., Laguesse, S., Pirotte, S., Hemphill, J., Rogister, F., Kruzy, N., Sacheli, R., Moonen, G., et al. (2014). MicroRNA targeting of CoREST controls polarization of migrating cortical neurons. Cell Rep. *7*, 1168–1183.

Walkinshaw, E., Gai, Y., Farkas, C., Richter, D., Nicholas, E., Keleman, K., and Davis, R.L. (2015). Identification of genes that promote or inhibit olfactory memory formation in *Drosophila*. Genetics *199*, 1173–1182.

Wang, Y., Wright, N.J., Guo, H., Xie, Z., Svoboda, K., Malinow, R., Smith, D.P., and Zhong, Y. (2001). Genetic manipulation of the odor-evoked distributed neural activity in the *Drosophila* mushroom body. Neuron *29*, 267–276.

Wightman, B., Ha, I., and Ruvkun, G. (1993). Posttranscriptional regulation of the heterochronic gene lin-14 by lin-4 mediates temporal pattern formation in *C. elegans*. Cell *75*, 855–862.

Yu, D., Keene, A.C., Srivatsan, A., Waddell, S., and Davis, R.L. (2005). *Drosophila* DPM neurons form a delayed and branch-specific memory trace after olfactory classical conditioning. Cell *123*, 945–957.

Yu, D., Akalal, D.B., and Davis, R.L. (2006). *Drosophila* α/β mushroom body neurons form a branch-specific, long-term cellular memory trace after spaced olfactory conditioning. Neuron *52*, 845–855.

Yu, H., Wu, M., Zhao, P., Huang, Y., Wang, W., and Yin, W. (2015). Neuroprotective effects of viral overexpression of microRNA-22 in rat and cell models of cerebral ischemia-reperfusion injury. J. Cell. Biochem. *116*, 233–241.